

Lamin A/C-regulated cysteine catabolic flux modulates stem cell fate through epigenome reprogramming

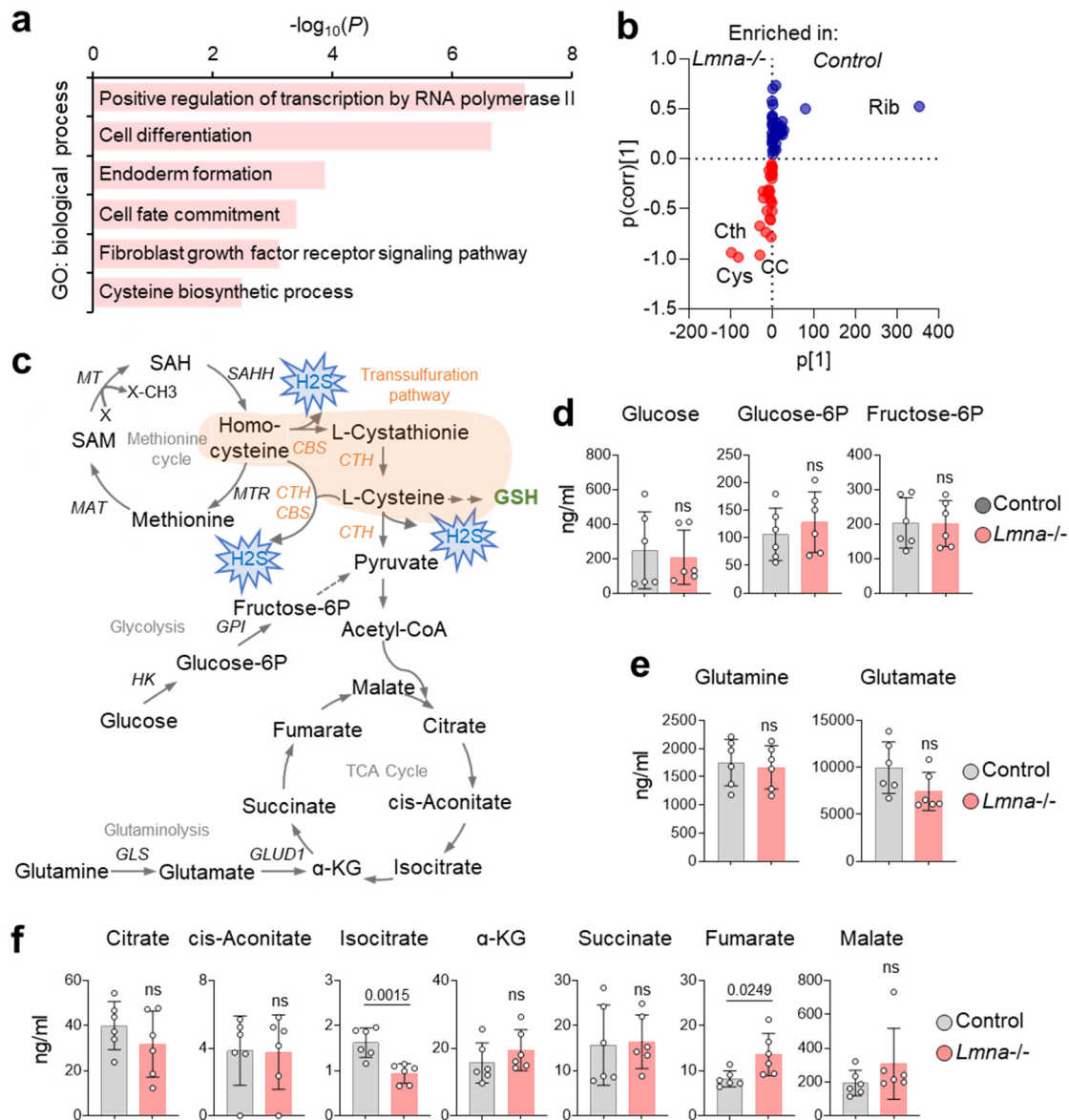
In the format provided by the
authors and unedited

Table of Contents

1. Supplementary Figures

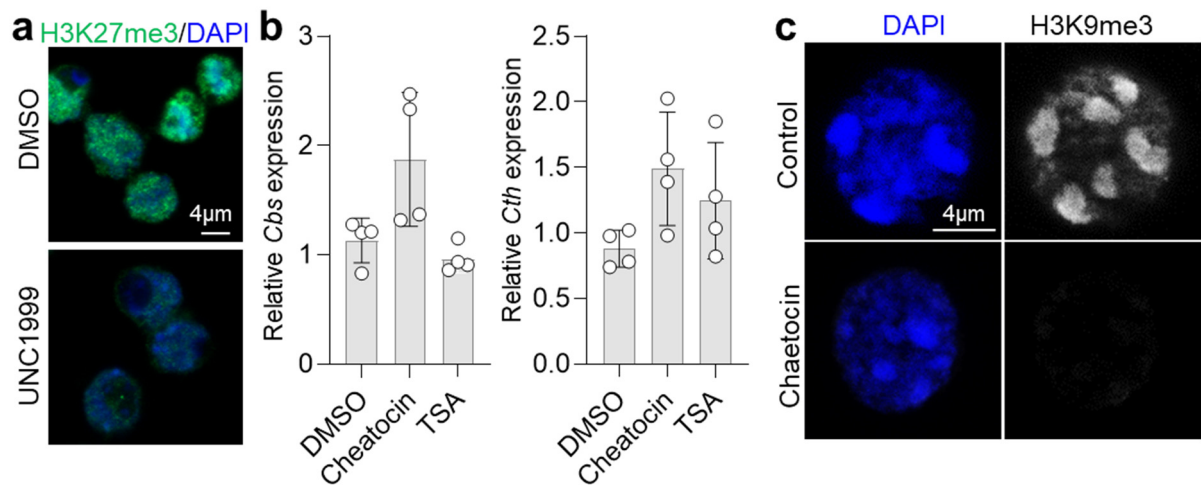
- Supplementary Fig. 1. Increased cysteine metabolism in *Lmna*^{-/-} mESCs.
- Supplementary Fig. 2. Impact of Ezh1/2, Suv39h1, and HDAC inhibition on *Cth* and *Cbs* expression.
- Supplementary Fig. 3. Lamin A/C-dependent CTH and CBS activation drives the transition from naïve to primed pluripotency.
- Supplementary Fig. 4. Enzyme activity of class I HDACs in control and *Lmna* mutant mESC.
- Supplementary Fig. 5. Impact of cysteine import on lamin A/C-dependent genes.
- Supplementary Fig. 6. CBS/CTH activation alters chromatin accessibility, 3D genome interactions and transcription of lamin A/C-dependent genes.

2. FACS gating strategy



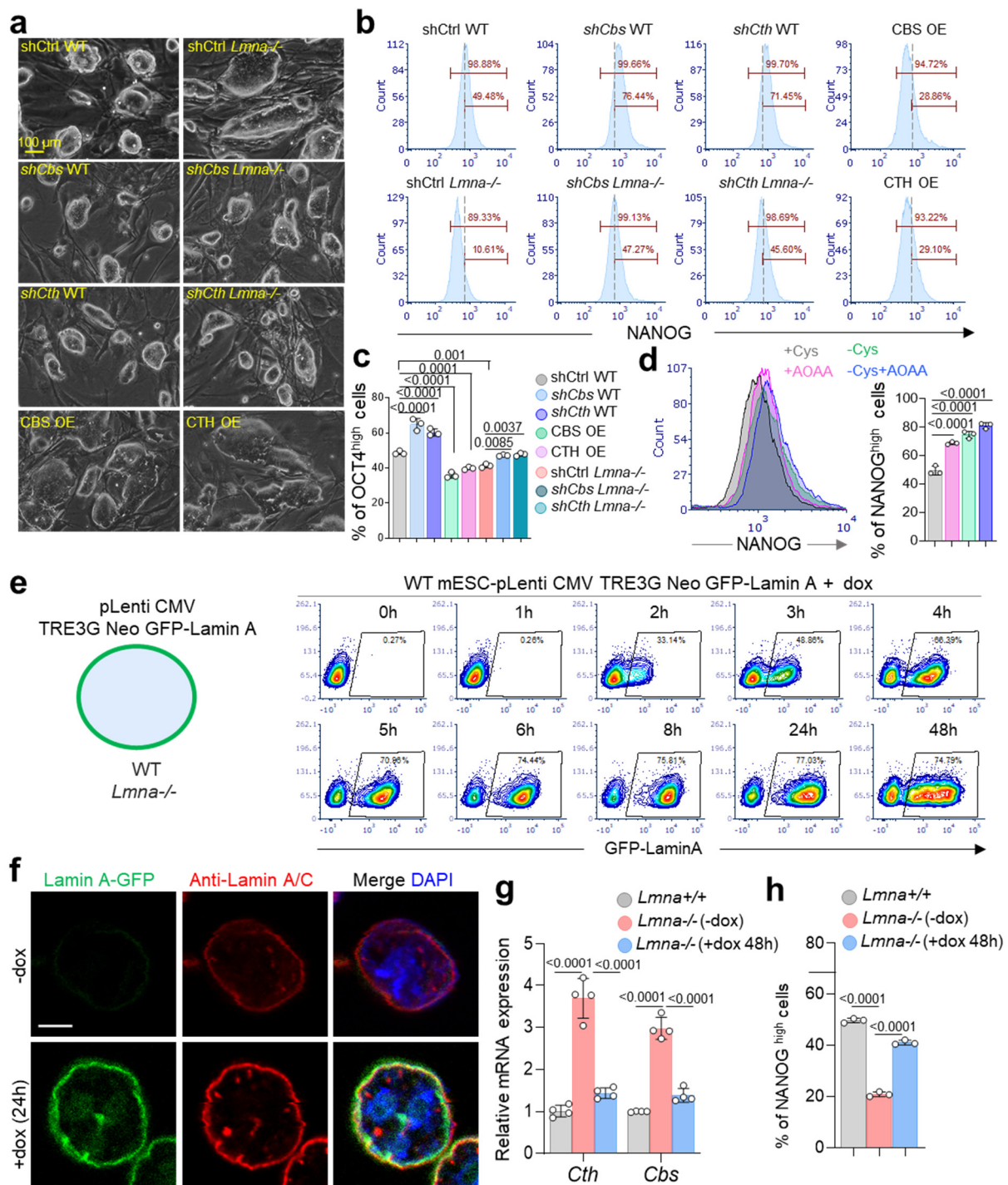
Supplementary Fig. 1. Increased cysteine metabolism in *Lmna*^{-/-} mESCs.

a, GO analysis of genes upregulated in *Lmna*^{-/-} mESCs. Significance was generated from DAVID with a one-sided Fisher's exact test. **b**, OPLS-DA S-plot of the most abundant metabolites contributing to the difference between *Lmna*^{-/-} and control groups. Annotations highlight metabolites deprived (blue dots) or accumulated in *Lmna*^{-/-} mESCs (red dots). Rib: ribose; Cys: cysteine; Cth: cystathionine; CC: Cystine. **c**, Schematic representation of the methionine cycle, the transsulfuration, glycolysis, glutaminolysis pathways and the TCA cycle. **d-f**, Intracellular level of metabolites associated with glycolysis (**d**), glutaminolysis (**e**) and TCA cycle (**f**) in control and *Lmna*^{-/-} mESCs. *n*=6 biological replicates. Data are presented as mean ± SD. Differences in **d-f** were assessed using an unpaired two-tailed Student's *t*-test. ns: not significant.



Supplementary Fig. 2. Impact of Ezh1/2, Suv39h1, and HDAC inhibition on *Cth* and *Cbs* expression.

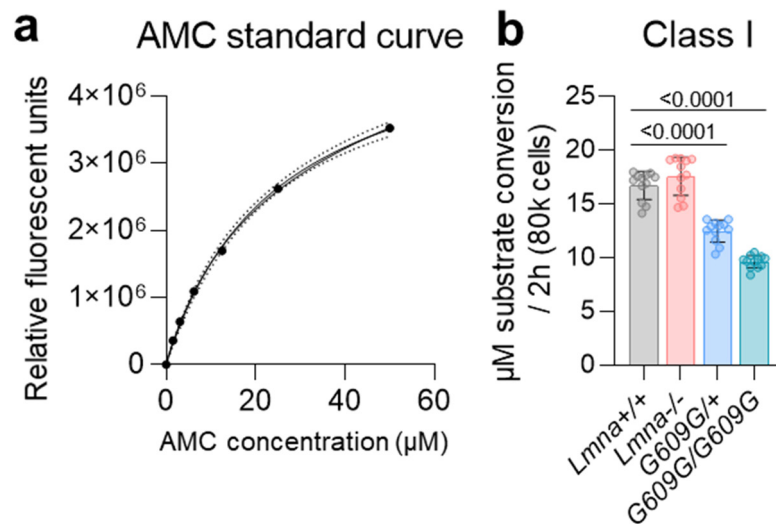
a, Immunostaining for H3K27me3 (green) and DAPI (blue) in WT mESCs treated with DMSO or the Ezh1/2 inhibitor UNC1999. **b**, Relative mRNA expression of *Cbs* and *Cth* in WT mESCs treated with DMSO, the Suv39h1 inhibitor chaetocin, or the HDAC inhibitor TSA. $n=4$ biological replicates. **c**, Immunostaining for H3K9me3 (green) and DAPI (blue) in WT mESCs treated with DMSO or the Suv39h1 inhibitor chaetocin. Data in **b** represent mean \pm SD. Differences were assessed using one-way ANOVA with Tukey correction.



Supplementary Fig. 3. Lamin A/C-dependent CTH and CBS activation drives the transition from naïve to primed pluripotency.

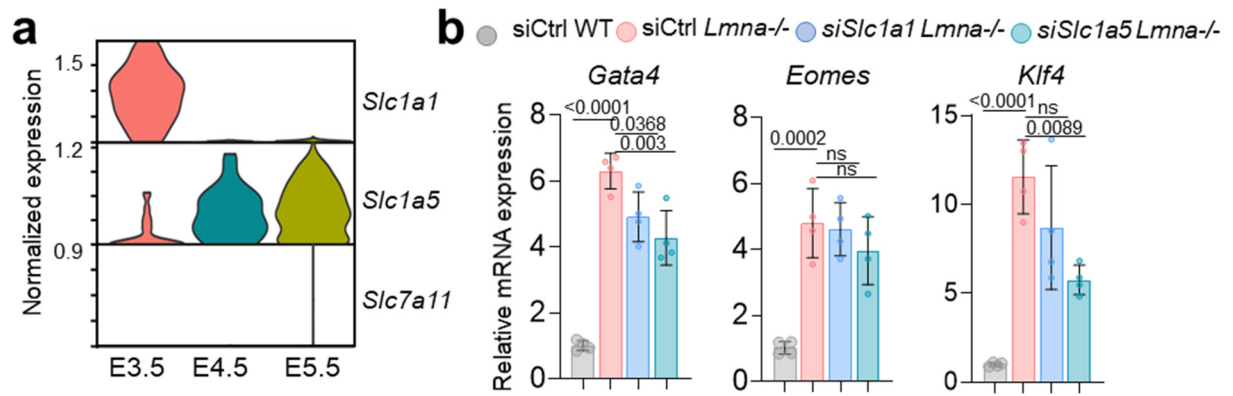
a, Phase contrast images showing colony morphology of control and *Lmna*^{-/-} mESCs after shRNA mediated silencing with control shRNA or shRNA against *Cth* or *Cbs* as well as CTH OE or CBS OE mESCs. Scale bar, 100 μ m. **b**, Representative histograms showing FACS analysis of NANOG^{high} cells in control and *Lmna*^{-/-} mESCs after shRNA mediated silencing with control shRNA or shRNA against *Cth* or *Cbs* as well as CTH OE or CBS OE mESCs. n=4 biological replicates. **c**, Percentage of cells highly expressing OCT4 (OCT4^{high}) determined by

FACS analysis of control and *Lmna*^{-/-} mESCs after shRNA mediated silencing with control shRNA or shRNA against *Cth* or *Cbs* as well as CTH OE or CBS OE mESCs. n= 3 biological replicates. **d**, Representative histograms showing FACS analysis (left) and percentage of NANOG^{high} cells (right) in mESCs cultured in standard medium, medium depleted of cysteine either not treated or treated with 100 μ mol/L AOAA for 48h. n= 3 biological replicates. **e**, Schematic representation of the generation of doxycycline-inducible lamin A overexpression in wild-type (WT) and *Lmna*^{-/-} mESCs (top), and time course FACS analysis of lamin A-GFP expression in wild-type murine E14-NKX2-5-EmGFP mESCs overexpressing the pLenti CMV TRE3G Neo GFP-Lamin A following treatment with 1 μ g/mL doxycycline. **f**, Immunostaining of lamin A-GFP, total lamin A/C (red), and DAPI (nuclei, blue) following 24h treatment with 1 μ g/mL doxycycline of WT murine E14-NKX2-5-EmGFP mESCs overexpressing the pLenti-CMV-TRE3G-Neo-GFP-Lamin A plasmid. Scale bar, 4 μ m. **g**, **h**, qPCR analysis of *Cbs* and *Cth* mRNA levels (**g**, n=4 biological replicates) and percentage of NANOG^{high} cells determined by FACS (**h**, n=3 biological replicates) in control mESCs and *Lmna*^{-/-} overexpressing the pLenti-CMV-TRE3G-Neo-GFP-Lamin A plasmid after 48 hours of treatment without or with 1 μ g/mL doxycycline. Data in **c**, **d**, **g** and **h** represent mean \pm SD. Differences in **c**, **d**, **g** and **h** were assessed using one-way ANOVA with Tukey correction.



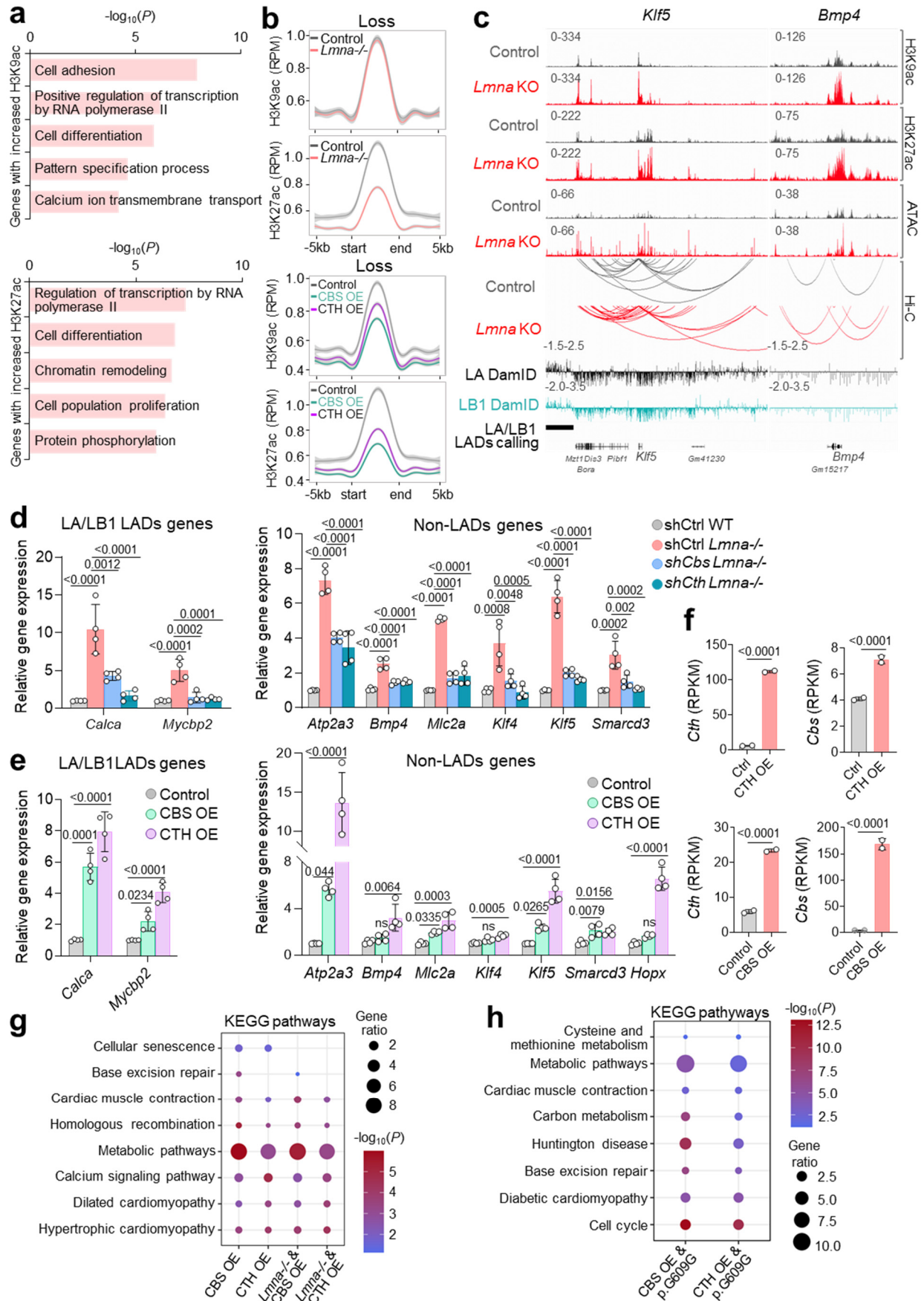
Supplementary Fig. 4. Enzyme activity of class I HDACs in control and *Lmna* mutant mESC.

a, Standard curve of AMC fluorescence used for quantification of HDAC activity. **b**, Class I HDACs activity measured in control, *Lmna*^{-/-}, *Lmna*^{G609G/+} and *Lmna*^{G609G/G609G} mESC. n=12 biological replicates. Data in **b** represent mean \pm SD. Differences were assessed using one-way ANOVA with Tukey correction.



Supplementary Fig. 5. Impact of cysteine import on lamin A/C-dependent genes.

a, Violin plots showing expression levels of cysteine transporters in preimplantation (E3.5 and E4.5) and postimplantation (E5.5) stage mouse embryos. **b**, Relative mRNA expression of the genes upregulated in *Lmna*^{-/-} mESCs after siRNA mediated silencing with control siRNA or siRNA against *siSlc1a1* or *siSlc1a5*. n= 4 biological replicates. Data in **b** represent mean ± SD. Differences were assessed using one-way ANOVA with Tukey correction. ns: not significant.



Supplementary Fig. 6. CBS/CTH activation alters chromatin accessibility, 3D genome interactions and transcription of lamin A/C-dependent genes.

a, GO analysis of genes showing a significant increase in H3K9ac (top) or H3K27ac (bottom) in *Lmna*^{-/-} compared to control. Log₂ fold change ≥ 0.58 ; p-value < 0.05 . **b**, Normalized H3K9ac ChIP-seq and H3K27ac ChIP-seq signal intensity in control (grey) and *Lmna*^{-/-} ESCs (red) or in control, CBS OE (green) and CTH OE mESCs (purple) at ATAC-seq peaks exhibiting decreased (loss) chromatin accessibility in *Lmna*^{-/-} mESCs versus control mESCs. RPM: Reads Per Million mapped reads. Log₂ fold change ≤ -0.58 ; p-value < 0.05 . **c**, IGV tracks showing H3K9ac ChIP-seq, H3K27ac ChIP-seq, ATAC-seq, lamin A (LA) DamID, lamin B1 (LB1) DamID and significant genomic interactions at H3K9ac and H3K27ac peaks determined by Hi-C in control (grey) and *Lmna*^{-/-} (red) mESCs at *Klf5* and *Bmp4* gene loci. **d**, Relative mRNA expression of the genes located in LA/LB1 LADs or outside of LADs (non-LADs) in control and *Lmna*^{-/-} mESCs after shRNA mediated silencing with control shRNA or shRNA against *Cth* or *Cbs*. n= 4 biological replicates. **e**, Relative mRNA expression of the genes located in LA/LB1 LADs or outside of LADs (non-LADs) in control, CTH OE and CBS OE mESCs. n= 4 biological replicates. **f**, Expression of *Cth* and *Cbs* in RNA-seq datasets of control, CBS or CTH OE mESCs. n=2 biological replicates. RPKM: reads per kilobase of transcript per million mapped reads. Significance was assessed using DESeq2 with a two-sided Wald test. **g**, Dot-plot representation of KEGG pathway analysis of genes upregulated in CTH OE and CBS OE mESCs or genes upregulated upon CTH OE or CBS OE and in *Lmna*^{-/-} mESCs. Log₂ fold change ≥ 0.58 ; p-adjusted value < 0.05 . **h**, Dot-plot representation of KEGG pathway analysis of genes both downregulated in *Lmna*^{G609G/G609G} mESC and upregulated in CTH OE or CBS OE mESC. Log₂ fold change ≤ -0.58 , ≥ 0.58 ; p-adjusted value < 0.05 . Data in **d-f** are presented as mean \pm SD. Differences in **d** and **e** were assessed using one-way ANOVA with Tukey correction. Significance in **a**, **g** and **h** was generated using DAVID with a one-sided Fisher's exact test. ns: not significant.

FACS gating strategy

